

4<sup>th</sup> International Conference on Advanced Composite Materials in Bridges and Structures  
4<sup>ième</sup> Conférence Internationale sur les matériaux composites d'avant-garde pour ponts et charpentes  
Calgary, Alberta, July 20 – 23, 2004 / 20 – 23 juillet 2004

## PUNCHING SHEAR STRENGTH OF GFRP REINFORCED DECK SLABS IN SLAB-GIRDER BRIDGES

T.K. Hassan and S.H. Rizkalla

Department of Civil, Construction and Environmental Engineering, North Carolina State University  
Centennial Campus, CFL, Campus Box 7533, Raleigh, NC, USA 27695-7533

[tarek\\_mohamed@ncsu.edu](mailto:tarek_mohamed@ncsu.edu)

[sami\\_rizkalla@ncsu.edu](mailto:sami_rizkalla@ncsu.edu)

R. Rochelle

North Carolina Department of Transportation

Raleigh, NC, USA 27699

[rdrochelle@dot.state.nc.us](mailto:rdrochelle@dot.state.nc.us)

**ABSTRACT:** Punching shear failure normally occurs in reinforced concrete slabs subjected to concentrated loads and particularly in concrete bridge decks due to development of an internal arching action within the system. Ongoing research revealed that the governing mode of failure for concrete bridge decks is not flexure and using flexural design method usually led to artificial high levels of steel reinforcement. This paper presents results of non-linear finite element formulation of typical concrete bridge decks reinforced with different types and configurations of FRP bars to study their effectiveness under service and ultimate limit states. The accuracy of the non-linear finite element analysis is demonstrated using independent test results conducted by other researchers. The behavior of the FRP-reinforced bridge decks was compared to that of the conventional bridge deck reinforced with steel reinforcement. The fundamental behavior of concrete bridge deck slabs is reviewed. A comparison between flexural and punching shear design concepts for concrete bridge deck slabs is presented.

### 1. INTRODUCTION

Extensive research into the behavior of concrete bridge deck slabs led to the conclusion that the primary structural action by which these slabs resist concentrated wheel loads is not flexure, as traditionally believed, but a complex internal membrane stress state referred to as internal arching [1-2]. Due to typical high rigidity of bridge girders and high thickness-to-span ratio of typical bridge deck slabs, the load mechanism developed into the slab creates an arch action rather than flexural behavior mechanism to resist the applied wheel loads. Several researchers indicated that the bottom reinforcements of the bridge deck slab act as ties for the arch action mechanism rather than flexural reinforcement for the positive moments. This paper demonstrates that the effect of the top reinforcement in bridge deck slabs is insignificant and is mainly needed to control shrinkage and temperature stresses as well as to achieve a better distribution for the localized concentrated stresses due to the applied concentrated loads [1-3].

## 2. ANALYTICAL MODELING

### 2.1 Validation of the Model

The finite element modeling described in this paper was conducted using the ANACAP program (Version 2.1) [4]. The reinforcing bars are modeled as individual sub-elements embedded within the concrete elements. The stiffness of the bars is added to the stiffness of the concrete element. The concrete is modeled using 20-node brick elements with a 2x2x2 reduced Gauss integration scheme. Each of the twenty nodes in any brick element has three translational degrees of freedom. The analysis is conducted using an incremental-iterative solution procedure, in which the load is incrementally increased up to failure. More details about the constitutive relations employed in ANACAP can be found elsewhere [5]. The applicability of non-linear finite element analysis to predict the punching shear behavior of concrete bridge decks is demonstrated by modeling a concrete deck slab supported on two steel girders and tested by El-Gamal et al., 2003 [6]. As illustrated in Fig. 1, the test consisted of 200 mm thick deck slab supported on two steel girders spaced by 2.0 m center-to-center. The ends of the slab were restrained by bolting them to the supporting steel girders through holes in the slab. The slab had a 50 mm long cantilever overhang beyond the edge of each flange of the steel girders that was not included in the analysis. The slab was loaded up to a load level of 250 kN and unloaded and then reloaded up to failure [6]. The load was applied as a concentrated load acting on an area of 250x600 mm to simulate the effect of a truck wheel load. The slab was reinforced with No.16 GFRP bars spaced by 200 mm in all directions except the bottom reinforcement in the main direction which consisted of No.16 GFRP bars spaced every 125 mm as shown in Fig. 1.

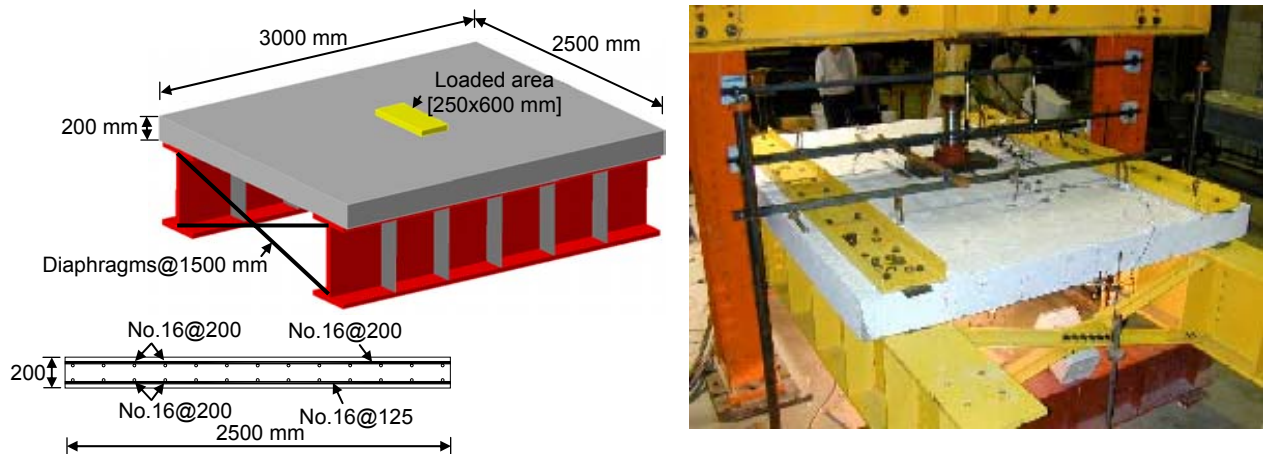


**Fig. 1 Bridge Deck Model [El-Gamal et al., 2003]**

The GFRP bars have an elastic modulus and tensile strength of 44 GPa and 675 MPa, respectively. The average concrete compressive strength was 50 MPa [6]. Due to symmetry, one quarter of the bridge deck slab was modeled and the slab thickness was divided into four layers as shown in Fig. 2. The steel girders were modeled by providing vertical translational restraints to the deck slab along the length of the web and at the locations of vertical stiffeners. The predicted load-deflection behavior using finite element analysis compared to the experimental results is shown in Fig. 3. The predicted load-deflection behavior of the bridge deck model compared very well with the measured values up to failure. The difference in deflections could be due to the small deflections of the stiff steel girders which were ignored in the analysis. The punching shear failure criterion developed by Kinnunen and Nylander, 1960 [7] was adopted in the non-linear finite element analysis. The punching load is determined when the circumferential compressive strain of the concrete reaches a critical value of 0.0019 at a distance of  $B/2+y$  from the loaded area where  $B$  is the diameter of the idealized load area and  $y$  is the location of centre of rotation of concrete wedges causing punching failure and can be approximated by  $0.1d$  where  $d$  is the thickness of

the slab. [1, 7]. The predicted punching failure load overestimated the measured value by 5 percent. More verification examples of the finite element model can be found in [3].

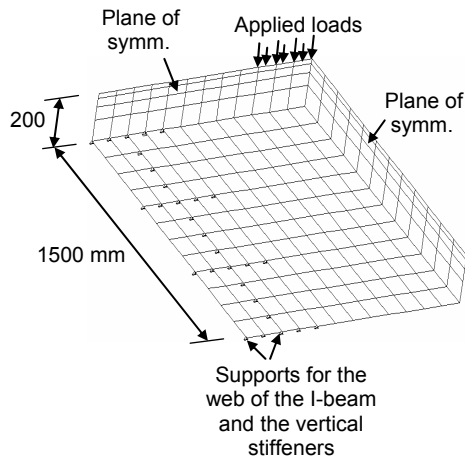


**Fig. 2 Mesh Dimensions**

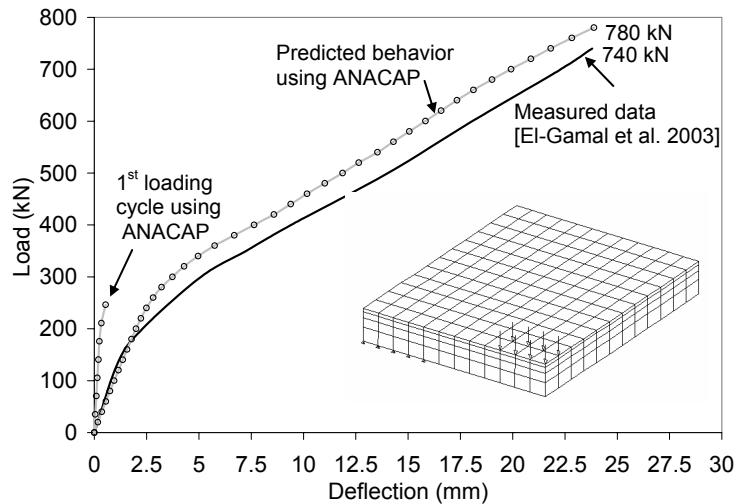


**Fig. 3 Predicted and Measured Load-Deflection Behavior**

## 2.2 Bridge Deck Slabs

A typical concrete bridge was selected to investigate the feasibility of using FRP bars as flexural reinforcement for continuous bridge deck slabs. The selected bridge is expected to be constructed in Macon County, North Carolina, USA in 2004. Traditional design using steel reinforcement for the deck slab is based on flexural theory according to the AASHTO bridge design specifications [8]. Reinforcement details for the bridge deck slab as recommended by the department of transportation are shown in Fig. 4.

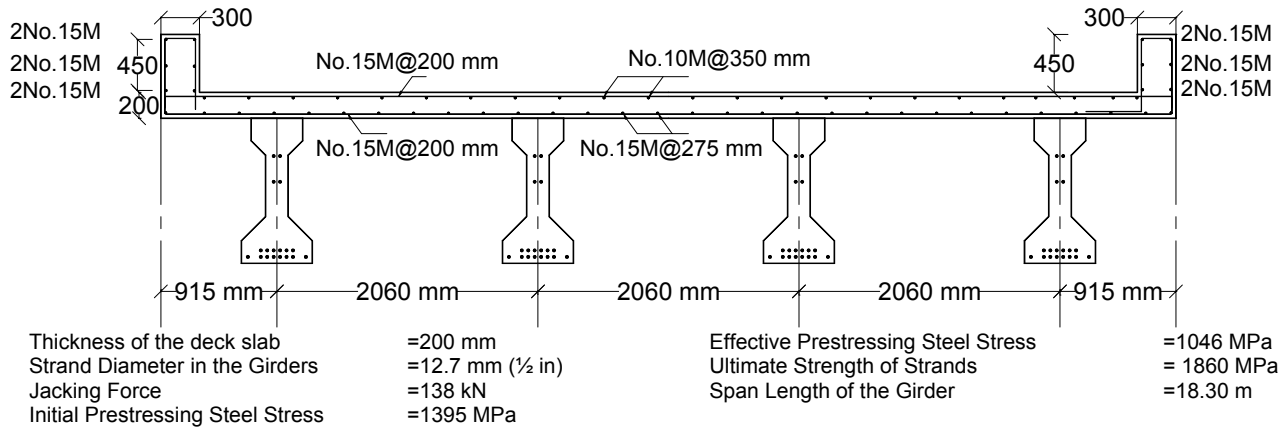


**Fig. 4 Typical Reinforcement Details for the Bridge Deck Slab [Macon County, NC, USA]**

Taking advantage of the symmetry of the bridge, only one quarter of the intermediate panel of the bridge was considered in the analysis as illustrated in Fig. 5a. An isometric view of the modeled portion of the bridge is shown in Fig. 5b. The compressive strength of the concrete slab was set to 25 MPa. The total slab thickness (200 mm) was divided into three equal layers. The cross-section of the AASHTO Type III girders was modified as shown in Fig. 5b to reduce the number of elements and to remain with a realistic execution time of the program. The new dimensions were selected to provide the same moment of inertia of the actual AASHTO Type III girders. The total number of elements used in the analysis was 960 elements. Two wheel loads representing an axle of a design truck were applied 4.6 m away from the girders' supports in the longitudinal direction of the bridge to induce the maximum negative moment in the

slab section in between the diaphragms. The transverse spacing between the wheels was set to 1.8 m as specified by the AASHTO bridge design specifications [8].

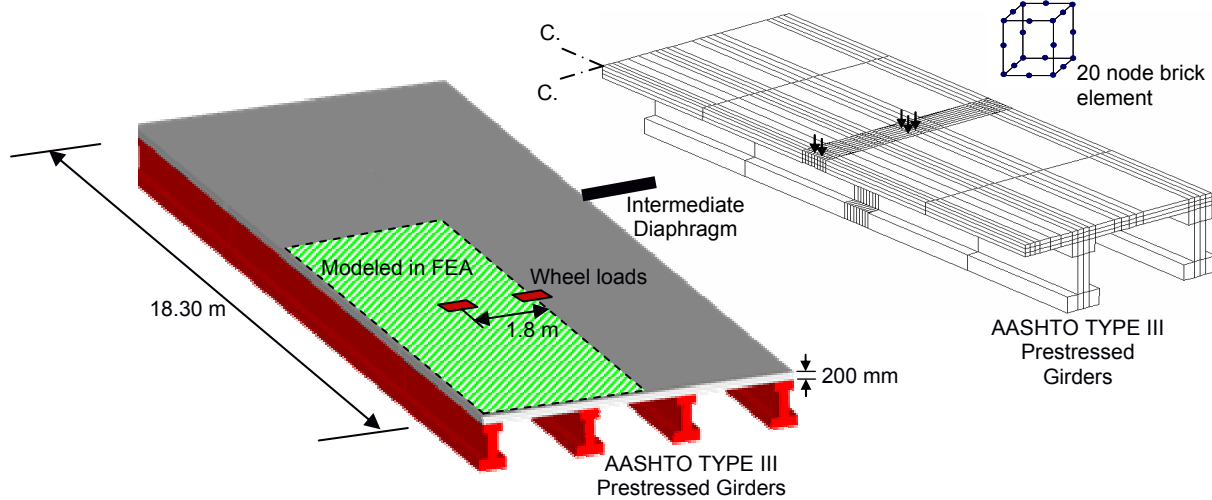


**Fig. 5a Modeling of the Bridge Deck Slab and AASHTO Girders**

**Fig. 5b Isometric View of the Modeled Portion of the Bridge**

Each wheel load was applied as a uniform pressure acting on an area of 250 mm x 500 mm. The loading sequence of the analysis accounted for various loading stages, including the stage where the prestressed girders were first installed to carry their own weight, followed by the application of fresh concrete during slab casting. Six different analytical simulations were carried out by varying the type and the configuration of the deck reinforcement. To check serviceability requirements after cracking of concrete, the slab in the analytical model was loaded up to a wheel load of 530 kN, then unloaded and reloaded again up to failure. Summary of the reinforcement configuration for different cases are given in Table 1.

**Table 1. Summary of the FEA for different reinforcement types and configurations**

Case #	Bottom Reinforcement		Top Reinforcement	
	Transverse	Longitudinal	Transverse	Longitudinal
1	Steel: No.15M@200mm ( $\rho=0.5\%$ )	Steel: No.15M@275mm ( $\rho=0.36\%$ )	Steel: No.15M@200mm ( $\rho=0.5\%$ )	Steel: No.10M@350mm ( $\rho=0.14\%$ )
2	Steel: No.15M@200mm ( $\rho=0.5\%$ )	Steel: No.15M@275mm ( $\rho=0.36\%$ )	GFRP: No.22@100mm ( $\rho=1.9\%$ )	GFRP: No.12@95mm ( $\rho=0.6\%$ )
3	Steel: No.15M@200mm ( $\rho=0.5\%$ )	Steel: No.15M@275mm ( $\rho=0.36\%$ )	GFRP: No.22@160mm ( $\rho=1.2\%$ )	GFRP: No.12@95mm ( $\rho=0.6\%$ )
4	GFRP: No.22@100mm ( $\rho=1.9\%$ )	GFRP: No.12@95mm ( $\rho=0.6\%$ )	GFRP: No.22@100mm ( $\rho=1.9\%$ )	GFRP: No.12@95mm ( $\rho=0.6\%$ )
5	GFRP: No.22@160mm ( $\rho=1.2\%$ )	GFRP: No.12@95mm ( $\rho=0.6\%$ )	GFRP: No.22@160mm ( $\rho=1.2\%$ )	GFRP: No.12@95mm ( $\rho=0.6\%$ )
6	GFRP: No.22@160mm ( $\rho=1.2\%$ )	GFRP: No.12@95mm ( $\rho=0.6\%$ )	GFRP: No.12@95mm ( $\rho=0.6\%$ )	GFRP: No.12@95mm ( $\rho=0.6\%$ )

- Failure was due to punching shear for all cases

- $\rho$  is the reinforcement ratio =  $\frac{\text{Area of reinforcement / unit width}}{\text{Unit width of the slab} \times \text{Thickness of the slab}}$

## 2.3 Results and Discussion

### 2.3.1 Case 1

The first case in the analytical modeling simulates the behaviour of conventional concrete bridge decks reinforced with steel reinforcement and designed according to the traditional flexural theory. The yield strength and modulus of elasticity of the steel reinforcement were set to 400 MPa and 200 GPa, respectively. Net slab deflection was based on the total deflection of the slab minus the girder's deflection. The predicted load-deflection behavior of the slab under the applied wheel loads is shown in Fig. 6. The behavior is linear up to initiation of flexural cracking, at a wheel load of 340 kN, followed by a non-linear behaviour up to failure. The predicted deflection of the slab under service loading conditions is equivalent to the span/3476, which is well below the value recommended by the AASHTO bridge specifications (span/800). The slab failed due to concrete crushing leading to punching shear failure with a corresponding concrete compressive strain of 0.0019 at a distance of B/2+y (260mm) from the loaded area. The maximum compressive strain in the concrete under the loaded area was 0.0045. The maximum compressive stresses in the concrete reached a value of 40 MPa which is 60 percent higher than the specified compressive strength. This is attributed to the concrete confinement due to the triaxial state of stresses under the loading area. The predicted wheel failure load due to punching shear was 685 kN. The predicted deflection of the slab was significantly increased after yielding of the bottom transverse steel reinforcement at a load level of 667 kN. The maximum tensile strain in the bottom transverse steel reinforcement at failure was 0.22 percent.

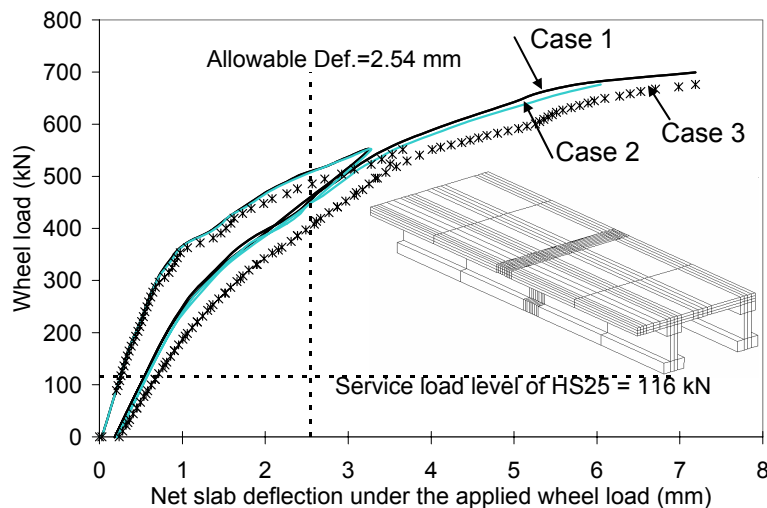


**Fig. 6 Predicted Load-Deflection Behavior for Cases 1, 2 and 3**

### 2.3.2 Case 2

To demonstrate the effect of the type of the top reinforcement on the deck behavior, the top steel reinforcement used in the first case of the analysis was replaced with GFRP reinforcing bars. The area of the GFRP bars was designed based on the traditional flexural theory ignoring the compressive membrane forces due to arching action. The top transverse reinforcement consisted of No. 22 GFRP bars spaced every 100 mm which represents an equivalent reinforcement ratio of 1.9 percent. The tensile strength and modulus of elasticity of the GFRP bars were 600 MPa and 41 GPa, respectively. The bottom steel reinforcement ratios in the transverse and longitudinal directions were kept constant as in case 1. The predicted load-deflection behavior, shown in Fig. 6, indicates similar behavior of the conventional steel-reinforced bridge deck up to failure. The predicted deflection values at service load level were identical in

both cases. The predicted failure load due to punching shear was 676 kN which is 1.3 percent less than that predicted for the deck slab reinforced with steel reinforcement.

### 2.3.3 Case 3

The influence of the reinforcement ratio of the top transverse reinforcement for bridge deck slabs was investigated in case 3 by placing 1.2 percent GFRP bars (No. 22 GFRP bars spaced every 160 mm) as top transverse reinforcement. The bottom steel reinforcement ratios in the transverse and longitudinal directions were kept constant as in case 1. The predicted load-deflection behavior of the three cases is shown in Fig. 6. The analysis indicates that reducing the top transverse reinforcement ratio by 37 percent has an insignificant effect on the behavior as well as on the punching shear capacity of bridge deck slabs.

### 2.3.4 Case 4

The behavior of continuous bridge deck slabs reinforced totally with GFRP reinforcing bars is studied in case 4. The top and bottom transverse reinforcement ratios were set to 1.9 percent. The top and bottom longitudinal reinforcement ratios were set to 0.6 percent. The predicted load-deflection behavior compared to that of the conventionally-designed deck slab using steel reinforcement is shown in Fig. 7. The same initial stiffness and cracking load were observed regardless of the reinforcement type and configuration. The maximum predicted deflection at service load level for the deck slab reinforced totally with GFRP bars was 7 percent higher than the corresponding value predicted for the deck slab reinforced with steel reinforcement (case 1). Nevertheless, the maximum predicted deflection in case 4 is still well below the limiting value recommended by the AASHTO bridge design specifications. The axial stiffness of the bottom transverse reinforcement is 30 percent less than that of the deck slab reinforced with steel reinforcement. The analysis indicates that increasing the axial stiffness of the bottom transverse reinforcement decreases the mid-span deflection of the deck slab considerably as shown in Fig. 7. The predicted punching shear carrying capacity in case 4 is 2 percent less than that of the deck slab reinforced with steel reinforcement. The decrease in ultimate load is due to the reduction of the compressive membrane forces induced by decreasing the axial stiffness of the reinforcement, which consequently decreases the punching shear capacity of the slab. Typical cracking pattern of the bridge deck slab at different loading stages is shown in Fig. 8. Principal compressive stresses at failure are illustrated in Fig. 9.

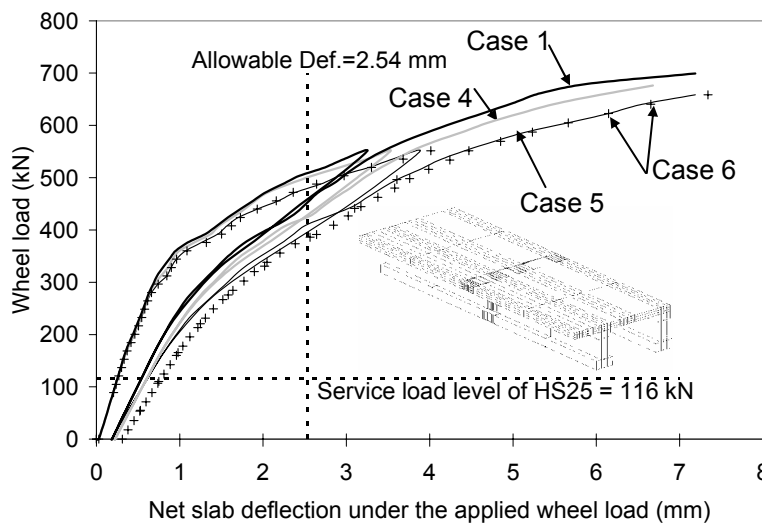


**Fig. 7 Predicted Load-Deflection Behavior for Cases 1, 4, 5 and 6**

### 2.3.5 Cases 5 and 6

Based on the results of the analysis for case 4 which demonstrates the excessive safety margins compared to code requirements at serviceability limit states, the reinforcement ratio of the top and bottom transverse GFRP reinforcing bars was further reduced to 1.2 percent in case 5. The top and bottom longitudinal reinforcement ratios were kept constant at 0.6 percent. Fig. 7 shows that reducing the top and bottom transverse reinforcement ratio by 37 percent, increases the deflection values at service load level by 4 percent. The predicted punching shear carrying capacity is 4 percent less than that the capacity of the bridge deck slab reinforced with steel reinforcement in case 1. In case 6, the same GFRP reinforcement configuration as in case 5 was used except for the top transverse reinforcement ratio, which was further reduced to 0.6 percent instead of 1.2 percent. Identical behavior was observed for cases 5 and 6 regardless of the top transverse reinforcement ratio as shown in Fig. 7. The analysis indicates that the behavior of the deck slab is controlled primarily by punching shear rather than flexure and therefore, the top reinforcement ratio has a minor effect on the punching shear capacity of continuous bridge deck slabs. The ultimate capacity was predicted by the AASHTO and OHBDC design codes [8,9]. None of these codes takes into account the effect of the reinforcement ratio on the punching shear capacity. The punching shear capacity as predicted by AASHTO and OHBDC was 570 and 623 kN, respectively. The predicted failure loads using both design codes underestimate the punching shear capacity of the concrete deck slab reinforced with steel reinforcement by 20 percent and 10 percent, respectively. This is attributed to the effect of the lateral restraint provided in continuous bridge deck slabs and not considered in the design codes.

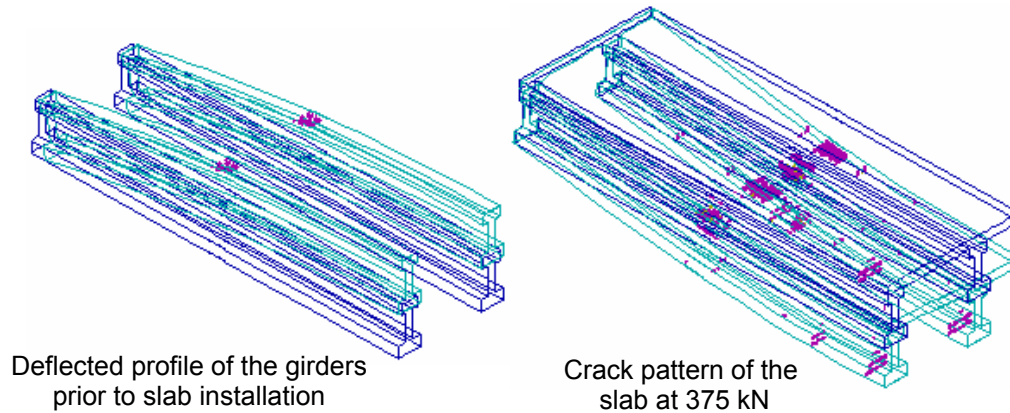


**Fig. 8 Cracking Pattern of the Bridge Deck Slab at Different Load Levels**

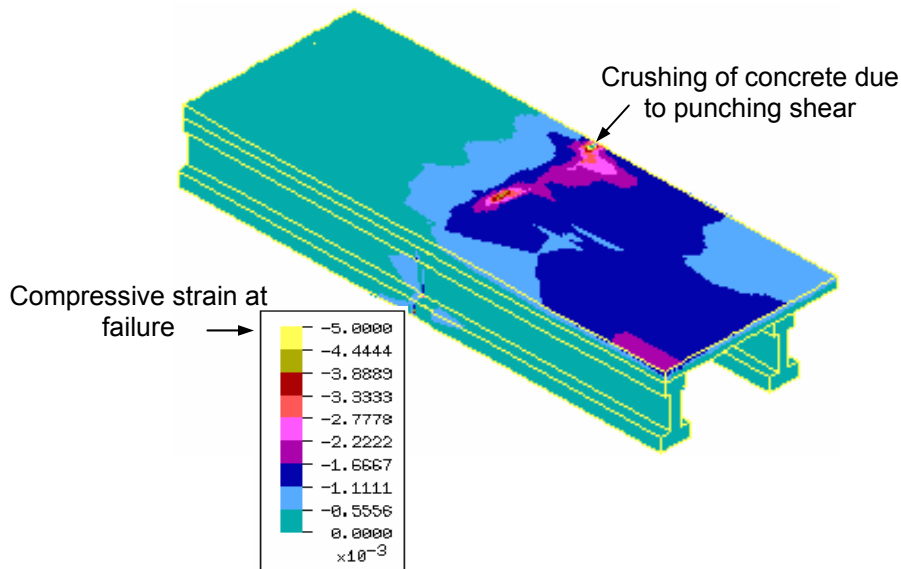


**Fig. 9 Typical Principal Compressive Strain Distribution of the Bridge Deck Slab at Failure**

### 3. DESIGN RECOMMENDATIONS AND CONCLUSIONS

Based on the results of the finite element analysis and practicability of constructing concrete bridges using FRP reinforcing bars, the proposed GFRP bottom transverse reinforcement ratio shall not be less than 1.2 percent. The top and bottom longitudinal GFRP reinforcement as well as the top transverse reinforcement shall not be less than 0.6 percent to resist shrinkage and temperature stresses. Using the proposed values for the reinforcement ratios will ensure that the deflections under service load level is well below the limiting value required by the AASHTO code. The maximum tensile stresses in the bottom and top transverse GFRP bars at service load level are 17 MPa and 16 MPa, respectively which are less than 20 percent of the ultimate tensile strength of the rebars. Consequently, creep rupture problem of GFRP bars is not a concern. Based on the results of the analysis, the following conclusions can be drawn:

1. Non-linear finite element analysis using ANACAP is capable of predicting the behaviour, ultimate load carrying capacity, and mode of failure of bridge deck slabs reinforced with different types of reinforcement.
2. Failure mode of continuous bridge deck slabs, having a span-to-depth ratio of 10 or less is due to punching shear. Traditional design procedures using flexural theory will provide unnecessary high levels of reinforcement.
3. The presence of top transverse reinforcement in bridge deck slabs has a negligible effect on the punching shear capacity.

### 4. ACKNOWLEDGEMENT

The authors wish to acknowledge the support of North Carolina Department of Transportation, National Science Foundation, award No. EEC-0225055 and National Science and Engineering Research Council of Canada.

### 5. REFERENCES

- [1] Mufti, A.A and Newhook, J.P., "Punching Shear Strength of Restrained Concrete Bridge Deck Slabs," *ACI Structural Journal*, 95, 4, 1998, pp 375-381.
- [2] Kuang, J.S. and Morely, C.T., "Punching Shear Behavior of Restrained Reinforced Concrete Slabs", *ACI Structural Journal*, 89, 1, 1992, pp 13-19.
- [3] Hassan, T., Abdelrahman, A., Tadros, G., and Rizkalla, S., "FRP Reinforcing Bars for Bridge Decks," *Canadian Journal for Civil Engineering* 27, 5, 2000, pp 839-849.
- [4] James, R. G., "ANACAP Concrete Analysis Program Theory Manual," Version 2.1, Anatech Corp., San Diego, CA, 1997.
- [5] Gerstle, K. H., "Material Modeling of Reinforced Concrete," *IABSE Colloquium on Advanced Mechanics of Reinforced Concrete*, Delft, Netherlands, 1981.
- [6] El-Gamal, S., El-Salakawy, E., and Benmokrane, B., "Shear Behavior of FRP-Reinforced Concrete Bridge Decks Under Concentrated Loads" *Proceedings of the Second International Workshop on Structural Composites for Infrastructure Applications*, Cairo, Egypt, Dec. 2003.
- [7] Kinnunen, S., and Nylander, H., (1960) "Punching of Concrete Slab without Shear Reinforcement," *Transactions of the Royal Institute of Technology*, Stockholm, Sweden, No. 158.
- [8] AASHTO, "Standard Specifications for Highway Bridges 1996", American Association of State Highway and Transportation Officials, Washington D.C.
- [9] OHBDC, 1991 "Ontario Highway Bridge Design Code", Ministry of Transportation of Ontario, Downsview, Ontario, Canada.